Phase stability and structural temperature dependence in powdered multiferroic $BiFeO_3$

R. Haumont,[1] Igor A. Kornev,[2,*] S. Lisenkov,[2] L. Bellaiche,[2] J. Kreisel,[3] and B. Dkhil[4]
[1]*Laboratoire de Physico-Chimie de l'Etat Solide, ICMMO, CNRS-UMR8182, Université Paris XI, 91405 Orsay, France*
[2]*Physics Department, University of Arkansas, Fayetteville, Arkansas 72701, USA*
[3]*Laboratoire Matériaux et Génie Physique (CNRS), Grenoble Institute of Technology, Minatec 38016 Grenoble, France*
[4]*Laboratoire Structures, Propriétés et Modélisation des Solides, Ecole Centrale Paris, CNRS-UMR8580, Grande Voie des Vignes, 92295 Châtenay-Malabry Cedex, France*

(Received 12 December 2007; revised manuscript received 9 September 2008; published 23 October 2008)

We report a temperature-dependent investigation of the multiferroic perovskite bismuth ferrite $BiFeO_3$ (BFO) by using x-ray powder diffraction together with differential scanning calorimetry measurements. Our results provide evidence that the paraelectric phase above T_c=820 °C is not cubic but distorted and can be well refined in a monoclinic $P2_1/m$ space group. An equivalent structure can be reconstructed based on the $C2/m$ monoclinic space group and by assuming two types of bismuth sites. The marked change of the cell volume at T_c provides evidence for the first-order nature of the $R3c$-to-$P2_1/m$ transition. The high-temperature $P2_1/m$ phase is centrosymmetric and characterized by (i) strong oxygen octahedra tilting along the b axis; (ii) the occurrence of antiferroelectric displacements of the Fe cations; and (iii) an interesting lamellar structure characterized by two different types of BiO_{12} cages. The temperature-induced lamellar structure suggests a significant electronic rearrangement in terms of chemical bonding, which in turn might condition anisotropic electronic properties. The occurrence of a lamellar structure provides also an understanding of why BFO decomposes suddenly at higher temperatures. Finally, an anomaly in the evolution of the cell parameters at T_N underlines the spin-lattice coupling in proximity of the magnetic transition.

DOI: 10.1103/PhysRevB.78.134108 PACS number(s): 61.05.cp

I. INTRODUCTION

Multiferroics, also called "ferroelectromagnets," are known for a long time as materials exhibiting at least both magnetic and polar order.[1] During the last few years, investigations on multiferroics have been renewed due to their intriguing physical properties and their potential applications for novel magnetoelectric thin film devices (magnetic memories for spintronics, tunable microwaves for filters, sensors and actuators for electromechanical systems, etc.).[2–5] This field of solid state science is a challenging field with important experimental and theoretical efforts to obtain a better understanding of the coupling mechanisms between the different order parameters. Multiferroic materials are also considered rare. Among them, $BiFeO_3$ (BFO) is the most studied and promising candidate,[2] considered as a holy grail,[6] as it exhibits "robust" multiferroic properties with coexistence of both antiferromagnetic (T_N=352 °C–370 °C) (Refs. 7–12) and ferroelectric (T_C=810 °C–830 °C) (Refs. 8 and 11–15) orders. Note that the precise value and nature of T_C has been debated for a long time as some pioneering works based on x-ray diffraction, dielectric measurements, conductivity, or dilatometric linear expansion have reported that the Curie temperature is rather close to 850 ± 15 °C,[16–18] whereas some others have proposed that this temperature is not associated to a transition toward a paraelectric cubic transition, and mentioned that the Curie transition occurs at even higher temperatures 875–880 °C.[19] At room temperature, bulk $BiFeO_3$ crystallizes in a rhombohedral symmetry with the $R3c$ space group. This structure is described (1) by Bi^{3+} and Fe^{3+} cations displaced along the [111] threefold polar axis and off centered with respect to the barycenter of the oxygen polyhedra, which in turn gives rise to ferroelectricity, and (2) rotations of adjacent oxygen FeO_6 octahedra around the [111] pseudocubic direction, corresponding to ($a^-a^-a^-$) tilt system in Glazer's notation.[20] The Fe^{3+} magnetic moments are ordered in a manner that a G-type antiferromagnetic ordering with a long-range cycloidal modulation (period of 640 Å) is obtained.[8,11,12] When synthesized as epitaxial thin films, both antiferromagnetic and ferroelectric subsystems of $BiFeO_3$ are drastically modified.[5] Whereas the resulting magnetic ordering of thin films is now fairly well understood,[21] some controversies remain on its crystal structure as rhombohedral,[22] tetragonal,[23] and monoclinic[3] structures have been proposed. Intensive researches were therefore carried out in order to better describe the phase diagram of BFO. As a result, it was recently demonstrated that the high-temperature phase (above T_C), in both thin film and bulk, is not a paraelectric cubic phase, as previously believed. A ferroelectric orthorhombic order-disorder phase ($P2mm$) resembling that of the classical ferroelectric $BaTiO_3$ was rather proposed at T_C, the transition to the cubic phase occurring at higher temperature, around 950 °C.[15] In parallel to this work, we investigate here in detail the structural evolution of bulk $BiFeO_3$ powders versus temperature. The purpose of this article is to experimentally investigate the structure of $BiFeO_3$ in a wide temperature range from −180 °C up to 1000 °C. The stability phases under air atmosphere and their structures are analyzed, and are also compared with predictions arising from the use of the recently developed effective Hamiltonian scheme of Ref. 13.

II. EXPERIMENT

$BiFeO_3$ powders were prepared by conventional solid-sate reaction using high-purity bismuth oxide Bi_2O_3 and iron ox-

 ©2008 The American Physical Society

ide Fe_2O_3 as starting compounds. The oxides were mixed in stoichiometric proportions, and calcined with a low-thermal treatment according to previous report in order to obtain the pure perovskite $BiFeO_3$, free from any impurity phases.[14] Diffraction patterns from $2\theta=5$ to 120 degrees with a step of 0.004 degrees were collected with a Philips *X*-celerator Bragg-Brentano diffractometer equipped with a copper source (monochromatic radiation $\lambda=1.54056$ Å), from −180 °C to 1000 °C under air atmosphere by using a cryostat and a furnace with an accuracy better than 0.1 °C and 2 °C, respectively. Various temperature steps were used with small ones of 10 °C around peculiar temperatures associated with phase/state transitions. Differential scanning calorimetry (DSC) (Setaram Labsys DSC) was used to follow the thermal stability of the different phases involved up to 1100 °C. Heating/cooling processes with a rate of 2.5 °C/min and several cycles were performed. Any appearance of endothermic or exothermic peaks is related to either structural or phase changes. The DSC measurement combined with the x-ray diffraction allowed to identify the different thermodynamic phases. Moreover, we have compared our experimental findings with theoretical predictions based on the first-principles-based effective Hamiltonian method of Ref 13. This approach reproduces well (i) the symmetry of the ground state, (ii) the Néel and Curie temperatures, and (iii) the intrinsic magnetoelectric coefficients. This scheme also predicts an overlooked phase above 1100 K that (a) is associated with antiferrodistortive motions, (b) exhibits improperlike dielectric behavior, and (c) is related to a first-order character ferroelectric transition with no group or subgroup relationship with the low-temperature phase.

III. RESULTS AND DISCUSSION

It is well known that at high-temperature $BiFeO_3$ becomes unstable due, e.g., to oxygen and/or bismuth volatility. Indeed, several experimental studies previously reported that the structure is unstable starting around ~820 °C–870 °C range of temperatures (depending on the authors) above which an irreversible chemical decomposition of the sample occurs[16] (in relation with the formation of parasitic phases often reported during sintering processes[24]).

Let us first describe the evolution of $BiFeO_3$ compound as a function of temperature up to 1100 °C. Figure 1 shows the DSC signal recorded during heating process. Three well-defined endothermic peaks can be seen at 820 °C, 930 °C, and 960 °C, and a broader and weaker one around 970 °C. After different heating/cooling processes, we evidenced only one reversible peak at 820 °C. Indeed, the inset of Fig. 1 shows that when the sample is heated up to 870 °C (which is below the second endothermic peak occurring at 930 °C) and then cooled down, a reversible exothermic peak with the same intensity/area than the endothermic one appears at 810 °C. The latter suggests a first-order phase transition. For the sake of clarity, we used the phase diagram from[25] that describes rather well the changes detected on the DSC data to describe the phases' stability [see Fig. 2(a)].

Figure 2(b) displays diffraction patterns for some specific temperatures noted on the phase diagram [Fig. 2(a)]. At room

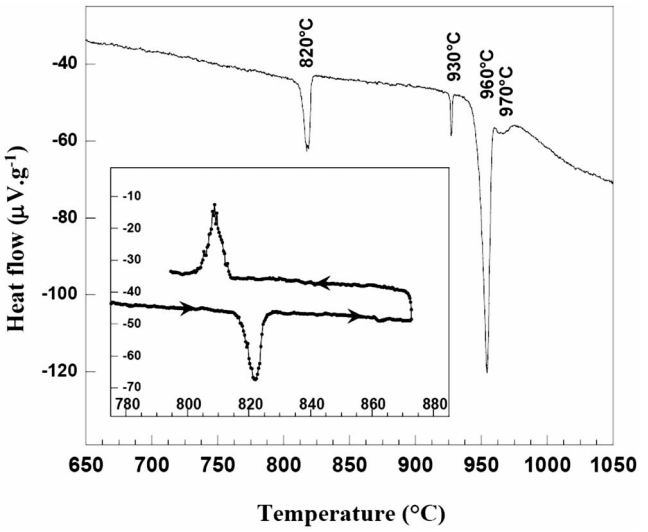

FIG. 1. DSC signal versus temperature in a BFO powder. Inset: zoom around the ferroelectric transition at 820 °C versus increasing and decreasing temperatures.

temperature and temperatures lower than 820 °C (e.g., $T=620$ °C on pattern A), the diffraction pattern is well described by the $R3c$ ground state of $BiFeO_3$. No additional/impurity peaks were evidenced, showing the high quality of the synthesized powder. On heating above 820 °C (pattern B) the diffraction pattern exhibits main diffraction peaks with 2θ positions that are close to the low-temperature $R3c$ phase, but further to this we observe additional weak peaks (pointed with diamonds symbols in the figure). Several heating/cooling cycles were done, which confirmed that the phase transition at around $T_c=820$ °C is reversible and that the appearance or disappearance of weak peaks is related to this phase transition. Thus, the stable high-temperature phase exhibits undoubtedly a complex diffraction pattern consisting of both main and weak Bragg peaks. Furthermore, the Bragg peaks are not single, which excludes a cubic phase above T_c, in good agreement with Ref. 15. This noncubic phase will be discussed later in the text.

Upon further heating, an irreversible decomposition at 930 °C occurs and is characterized by the loss of the $BiFeO_3$ diffraction pattern and the appearance of a pattern characteristic of $Bi_2Fe_4O_9$ [see arrows in inset of Fig. 1(b), pattern C]. A slight increase in the background (see inset pattern C) due to amorphous scattering also suggests the appearance of a small amount of a liquid, as expected from the phase diagram of Ref. 25. It is worth recalling that $Bi_2Fe_4O_9$ is the main parasitic phase, which appears during the sintering process when the sintering temperature is too high. We have also observed that this phase appears spontaneously at 870 °C–880 °C (thus far below 930 °C) after a long-time annealing treatment, which highlights a thermodynamic-kinetic competition.

Another change occurs with a strong endothermic peak at 960 °C corresponding to a peritectic plateau. Just above 960 °C [Fig. 2(b), pattern D] the diffraction pattern displays a coexistence of $Bi_2Fe_4O_9$ with Fe_2O_3 (shown with star symbols) and a larger amount of liquid phase [see inset of Fig.

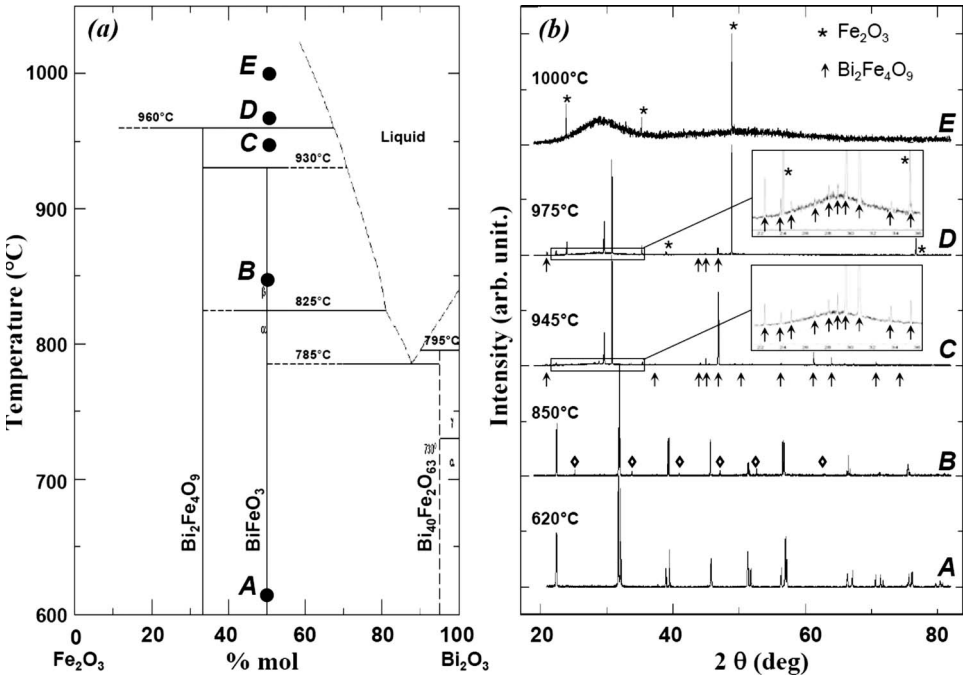

FIG. 2. Different crystalline phases and states of matter observed for $BiFeO_3$ versus temperature. Diamond symbols indicate the weak reflections which appear at the reversible transition $R3c \rightarrow P2_1/m$. Arrows and stars symbols localized the strongest diffraction reflections of $Bi_2Fe_4O_9$ and Fe_2O_3, respectively, during the irreversible decomposition of $BiFeO_3$.

2(b), pattern D]. Above around 970 °C corresponding to the weak and broad DSC signal, we observe a disappearance of $Bi_2Fe_4O_9$: the diffraction pattern shows a large amount of liquid in coexistence with the well-defined diffraction peak of Fe_2O_3 [Fig. 2(b), pattern E]. It is worth mentioning that by analyzing a $BiFeO_3$ single crystal we found the same thermal features and a total melting point reached at $T=1170$ °C, which is consistent with the phase diagram of Fig. 2(a) by extrapolating the liquidus line.

Let us now consider the structural phase transition around T_c. For each diffraction pattern recorded below the decomposition temperature around 930 °C, we have performed a Rietveld analysis by using the XND software.[26] Each diffraction pattern is refined using pseudo-Voigt peak-shape function including asymmetric broadening, linear interpolation for the background, and isotropic thermal factors. Below T_c, the structure is well described by the $R3c$ space group. Concerning the phase above T_c, in a first step of the structural analysis, because of the additional weak peaks (Fig. 2 and inset of Fig. 3), the classical perovskite symmetries—including cubic $Pm\text{-}3m$, tetragonal $P4mm$, orthorhombic $Bmm2$, rhombohedral $R3m$, and monoclinic Cm or Pm phases—are not able to well describe the whole diffraction pattern. Figure 3 shows the diffraction pattern recorded at 830 °C ($\sim T_c+10$ °C). It is worth noting that by using the classical previous symmetries the best refinement is obtained with the orthorhombic $Bmm2$ space group, which provides a rather good match between the observed and calculated strong Bragg peaks in good agreement with Ref. 15. However, the additional weak peaks (Fig. 2 and inset of Fig. 3) are not reproduced. In order to take into account the supplementary reflections evidenced in the diffraction pattern (see diamond symbols in Fig. 3), we have carefully indexed all the observed superstructure reflections. Using the double perovskite unit cell, we found that these weak peaks correspond to (oee) reflections (where o and e are *odd* and *even* Miller indexes, respectively), involving presence of clockwise and counter clockwise oxygen octahedra rotation. As the above T_c phase is expected to be paraelectric, noncentrosymetric groups in agreement with such tilt systems (*Cmcm*, *Pnma*,

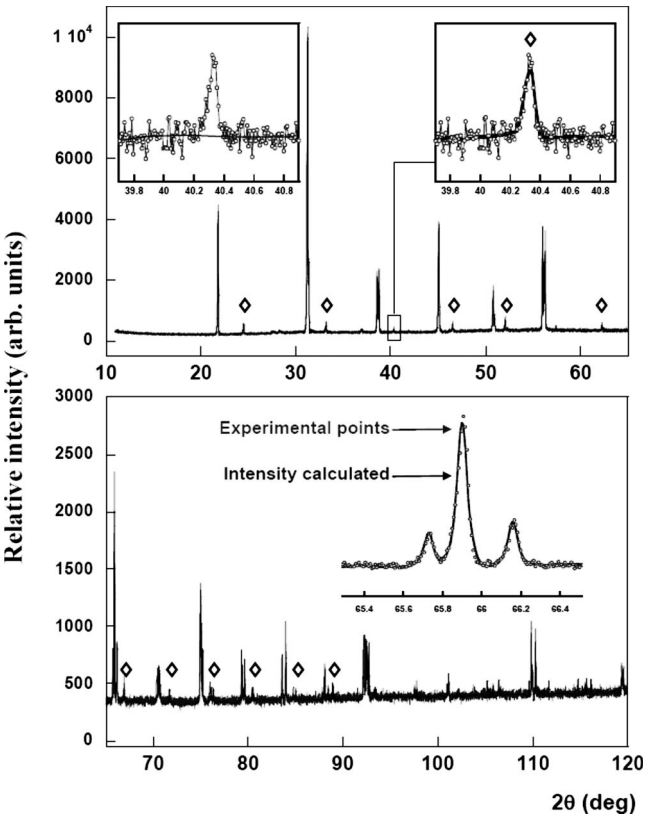

FIG. 3. Calculated (with the $P2_1/m$ symmetry) and observed diffraction pattern of $BiFeO_3$ ($T=830$ °C). A weak peak (diamond symbol) is enlarged in inset with orthorhombic (left, Ref. 15) and monoclinic symmetry (right).

TABLE I. Result of the Rietveld x-ray diffraction refinement on $BiFeO_3$ at 830 °C.

		$BiFeO_3$-830 °C-$P2_1/m$			
Lattice parameters	a(Å)	5.6148(3)			
	b(Å)	7.9725(1)			
	c(Å)	5.6467(1)			
	γ(°)	90.015(4)			
Position of Bi	x	0		$\frac{1}{2}$	
	y	0		0	
	z	0		$\frac{1}{2}$	
$B_{eq(Pb)}$(Å^2)		3.65		3.65	
Position of Fe	x	$\frac{1}{2}$		0	
	y	$\frac{1}{4}$		$\frac{1}{4}$	
	z	0		$\frac{1}{2}$	
$B_{eq(Fe)}$(Å^2)		2.87		2.87	
Position of O	x	$\frac{1}{2}$		0	
	y	0		0	
	z	0		$\frac{1}{2}$	
$B_{eq(O)}$(Å^2)		2.95		2.95	
Position of O	x	0.206727)	0.706727)	0.206727	0.706727)
	y	$\frac{1}{4}$	$\frac{1}{4}$	$\frac{1}{4}$	$\frac{1}{4}$
	z	0.1896(24)	0.1896(24)	0.6896(24)	0.6896(24)
$B_{eq(O)}$(Å^2)		3.33	3.33	3.33	3.33
	R_{wp}(%)	7.08			
	R_{exp}(%)	5.80			
	Rp (%)	5.84			
	Gof	1.22			
	R_{Bragg}(%)	3.56			

$P2_1/m$, and $P4_2/nmc$) were tested by Rietveld refinement; the best agreement matching between the observed and calculated profiles (Fig. 3) is obtained with the monoclinic $P2_1/m$ space group (Space Group SG $n°11$ of the International Tables of Crystallography[27]) with constrained oxygen atom positions. Indeed in such a phase, BFO is described with two kinds of Bi in Wyckoff positions (2*a*) and (2*d*), two Fe sites (2*e*) with ($x=\frac{1}{2}$, $y=1/4$, and $z=0$) and ($x=0$, $y=1/4$, and $z=\frac{1}{2}$), and six different sites for oxygen with positions (2*b*), (2*c*), and (2*e*). However because of the large number of refined variables for oxygen atoms, we had to constrain their positions as it is not reasonable to characterize properly this low structure symmetry using solely x-ray diffraction data. As a consequence, we therefore considered the positions for the oxygen atoms arising from those related to $C2/m$ space group, which is supergroup of $P2_1/m$, and particularly allows only three crystallographic sites (2*b*), (2*c*), and (8*j*) (SG $n°12$, with the origin taken on the $2/m$ site and the cell choice 2, let the $B112/m$ group), which is more suitable for the refinement with x-ray data. As a result, the final refinement obtained within the $P2_1/m$ space group with the oxygen atoms constrained is reported in Table I and gives rather good reliable factors. It is worth mentioning that we also performed a refinement with the $C2/m$ group by considering two Wyckoff positions *(2a)* and *(2d)* for Bi^{3+}, similarly to $P2_1/m$ group. Such refinement gives identical factors of reliability showing the similarity of both previous descriptions of the structure. Based on the x-ray diffraction data, it is therefore possible to describe the high-temperature phase of $BiFeO_3$ within either the $P2_1/m$ space group by constraining the oxygen positions or the $C2/m$ space group by imposing two different positions for the bismuth cations. As a result, the final $P2_1/m$ phase—as well as the $C2/m$—allows to reconstruct both the strong pseudocubic reflections and the weaker ones (see inset of Fig. 3). Interestingly, the lattice parameters at $T=830$ °C are $a_M=5.6148(3)$ Å, $b_M=7.9725(1)$ Å, $c_M=5.6467(1)$ Å, and $\gamma=90.015(4)°$, which are very close to a pseudotetragonal-like unit cell. Moreover this space group is centrosymmetric, which implies that the phase is *not* ferroelectric, unlike previously thought.[8,11,12] It was not possible to completely describe the antiferrodistorsive tilting system because of the large number of variables. The tilting system corresponds to $(a^-b^-c^+)$ in Glazer's notation[20] that we restricted artificially to $(a^-b^-c^0)$. Within this later system, the main tilting angle around the *b* axis is found to be equal to 11(1)°, which is very close to the one at room temperature [i.e., 13.8° (Ref. 28) around the rhombohedral main axis]. Nevertheless, further neutron diffraction data are strongly needed to better describe the oxygen tilting system of this monoclinic paraelectric phase.

This experimentally determined phase displays several similarities with that found in recent computations.[13] Indeed,

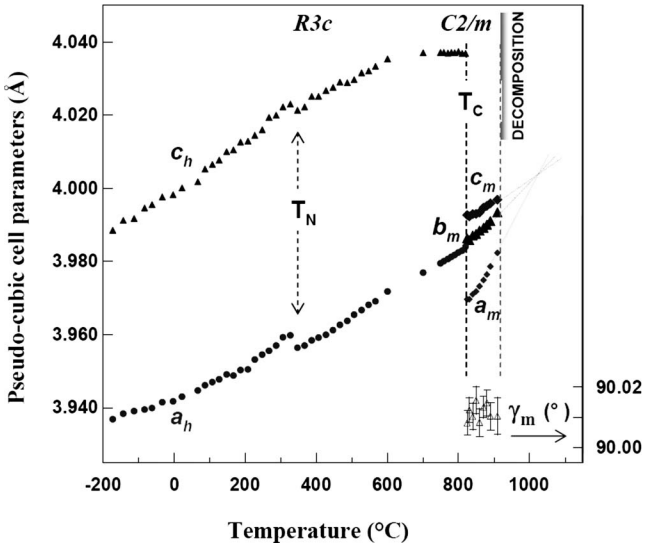

FIG. 4. Temperature-dependence evolution of the $R3c$ and the $P2_1/m$ cell parameters described in a pseudocubic cell ($a_h = a_H/\sqrt{2}$ and $c_h = c_H/2\sqrt{3}$, and $a_m = a_M/\sqrt{2}$, $b_m = b_M/2$, and $c_m = c_M/\sqrt{2}$). Error bars correspond to the size of the symbols.

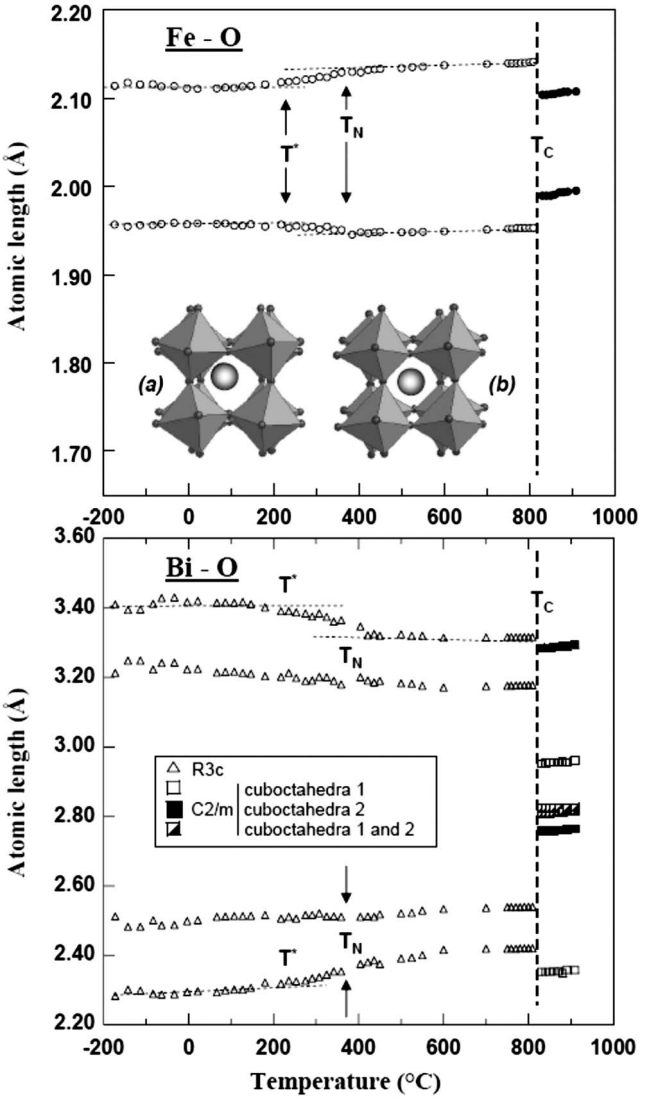

FIG. 5. Temperature dependence of Fe-O and Bi-O bonds in their respective FeO_6 octahedra and BiO_{12} cuboctahedra, in the rhombohedral and monoclinic phases.

these calculations demonstrated that the phase above T_c is not cubic, but is rather an antiferrodistortive paraelectric tetragonal phase with the space group $I4/mcm$, which is similar to that of the low-temperature phase of the classical $SrTiO_3$ compound. Actually $I4/mcm$ is one of the possible minimal supergroup of $C2/m$ space group, which underlines the proximity of these two phases.[29] Around 830 °C, our calculations give a tetragonal unit cell with an oxygen octahedra tilting angle of 10.3°, which is rather close to the experimental one. We also found experimentally that the final structure is actually much more complex and displays a lamellar character, described below, with BiO_{12} cuboctahedron strongly distorted and short (2.35 Å) and long (3.28 Å) Fe-O bonds. Such variation in chemical bonds may affect the conductivity properties of $BiFeO_3$, and an insulator-metal-like transition may be expected, as it was proposed in Ref. 15. It is also worth mentioning that micro-Raman diffusion performed on $BiFeO_3$ single crystals showed that this transition is accompanied by a marked and brutal increase in the background and the lost of the $R3c$ Raman spectra.[30] This signature might be due to incoming electron-phonon diffusion and thus may be a hint for an electric transition toward a more conductive phase. In a similar way, Kamba *et al.*,[31] by IR spectroscopy lead on BFO ceramics, also suggested such an improperlike nature of the phase transition at T_c. Note that such electronic rearrangement is not taken into account within our first-principles-based calculations and might well explain the discrepancy between the predicted $I4/mcm$ and the measured $P2_1/m$ symmetry for the phase above T_c.

Now, having established the space group symmetry, the lattice parameters and the Fe-O and Bi-O bond lengths can be extracted from the Rietveld refinements up to the decomposition temperature, as shown in Figs. 4 and 5, respectively. The values of a_h and c_h (i.e., hexagonal cell parameters a_H and c_H described in the pseudocubic cell) versus T agree well with the earlier data from Bucci *et al.*[16] By increasing the temperature, the c_h parameter (see Fig. 4) exhibits first a slowing down below T_c before decreasing suddenly and abruptly at T_c, whereas a_h parameter increases continuously and transforms into b_m above T_c with roughly the same thermal expansion coefficient through T_c. It is worth mentioning that the slowing down of the c_h parameter occurs around 600 °C, which corresponds to the minimum of the rhombohedral angle that was evidenced recently by synchrotron radiation diffraction.[32] Calculation of the unit-cell volume shows that the phase transition at T_c is therefore accompanied by a strong decrease in the volume with a variation $\Delta V/V$ of −1.4% as observed by Palai *et al.*[15] Such an important discontinuous change of the volume confirms the first-order nature of the phase transition and may also be related to an insulator-metal transition that is often associated with such volume changes. However, based on our calculations, the volume change around T_c is $\Delta V/V \approx -0.5\%$ and is al-

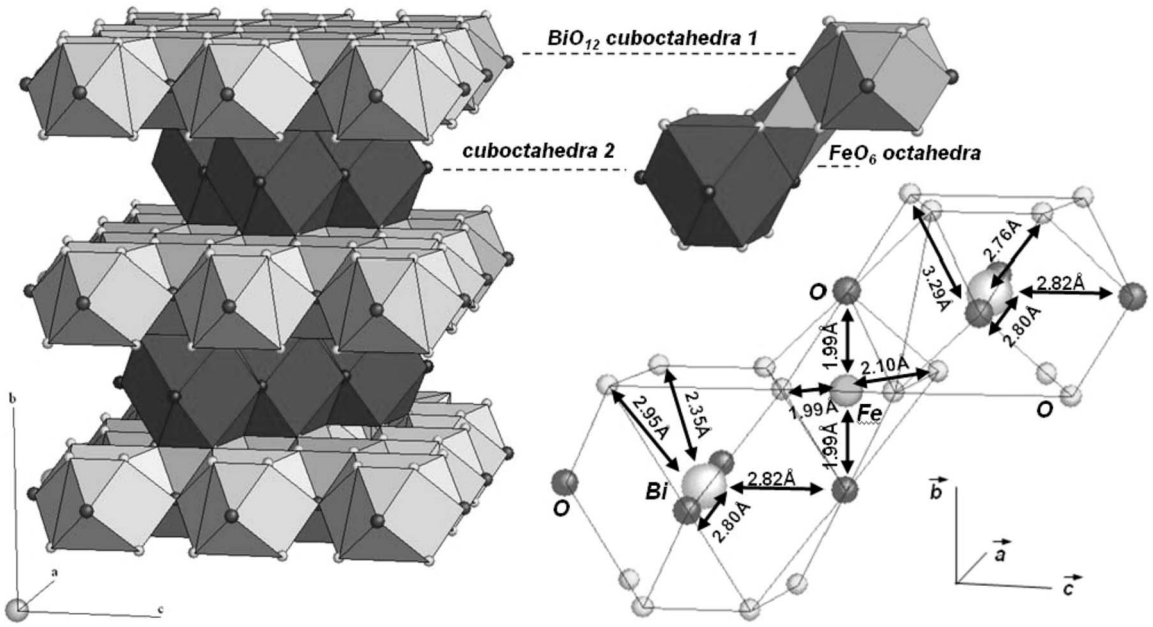

FIG. 6. $P2_1/m$ structure at 830 °C. The different lengths of chemical bonds in the two kinds of BiO_{12} cuboctahedron and in FeO_6 octahedra are emphasized.

ready rather important even without the consideration of any electronic rearrangement.

Moreover, as a consequence of the important volume change, a strong chemical rearrangement occurs. Indeed as shown in Fig. 5, the three short Fe-O bonds and the three long ones in the rhombohedral phase at room temperature are equal to 1.96 Å and 2.11 Å, which is in good agreement with a recent neutron diffraction investigation.[33] Note that this result provides also confidence in our x-ray analysis as the lengths found are similar to that determined from neutron diffraction technique (which is known to be a better-adapted technique to determine both the heavy- and light-atom positions in crystals such as $BiFeO_3$). At T_c, Fe-O bonds display a slight jump, then continuously and smoothly increase. Their values change very weakly with temperature; in a way they are reminiscent of the rhombohedral phase. The three short (1.96 Å) and three long (2.11 Å) bonds of the $R3c$ become four short (1.99 Å) and two long (2.10 Å) bonds. In this structure, antiparallel displacements are therefore evidenced as a Fe displacement within each oxygen octahedron is observed. However, the presence of the mirror plane perpendicular to the b axis causes an antiferroelectriclike network and the global polarization is expected to be zero in the whole structure. It is worth mentioning that a weak finite polarization value along the b axis is not completely excluded as the structure might be affected by the Bi and O nonstoichiometry. Regarding the Bi-O bonds, there is a strong change in bond lengths, and especially, we can distinguish two kinds of BiO_{12} cuboctahedron, built around the Bi($2a$) and Bi($2d$), respectively, with different chemical lengths (Fig. 6). These polyhedra have common length along a and c axis (two Bi-O bonds of 2.80 Å and two bonds of 2.82 Å, respectively). These two kinds of cuboctahedron, piled up in (a,c) planes and perpendicularly to the monoclinic b-axis, get a lamellar character to the structure. Such structural property involving the bismuth may also explain why and how the structure decomposes at high temperature. Indeed, we believe that temperature agitation can cause moving of Bi-planes ones on the others (like graphite) by breaking first long Bi-O bonds. However, to confirm this expectation, much more investigations are needed. Moreover, the increase in the electrical conductivity reported by Palai *et al.*[15] at T_c might be then mainly due to the contracting of Bi-O bond in the $P2_1/m$ phase in comparison with Bi-O length in $R3c$. Our experimental findings suggest also that the conductivity in the monoclinic phase is anisotropic, and should mainly occur in the (a,c) mirror plane of this lamellar structure. Figure 5 presents the temperature dependence of the different Bi-O bond observed in the structure (see also Fig. 6).

By increasing the temperature above T_c, the monoclinic phase evolves with a quasiconstant γ angle close to 90°, but always higher than 90° even in its error bars. Interestingly, the linear extrapolation of a_m, b_m, and c_m gives a single intersection at 1020 °C; a temperature where $BiFeO_3$ should be cubic if one assumes a second-order-like phase transition and, of course, if the sample would not have decomposed before. It is worth noting that the extrapolated cubic phase temperature is of the order of the one predicted from first principles that is around 1167 °C.[7]

Further inspection of both Figs. 4 and 5 also allows evidencing the Néel temperature T_N. Indeed a small jump occurs around 350 °C in a_h and c_h lattice parameters, which induces a variation in volume $\Delta V/V=0.21\%$. Below and above T_N, the cell parameters describe a quasilinear temperature evolution with close dilatation coefficients for a_h and c_h (respectively, equal to $4.5935\ 10^{-5}$ Å.°C^{-1} and $5.9566\ 10^{-5}$ Å.°C^{-1}). This result is in agreement with the earlier observation by Bucci *et al.*[16] and brings also a support to the strong spin-lattice coupling evidenced by Raman

spectroscopy.[30] It is remarkable that this temperature is also evidenced by the evolution of the bond length in Fig. 5 by weak but detectable linear deviation. Interestingly, another peculiar temperature, called T^* and close to 200 °C, was also evidenced by neutron diffraction.[32] Although the change is subtle, this temperature can be also evidenced on the lattice parameters, especially on a_h, and in the bond length as shown in Figs. 4 and 5 through an inflection point (see arrow). We suggest that through the crystal structure, the magnetic structure arranges itself continuously and slowly between T^* and T_N.

IV. SUMMARY

In conclusion, in this work we have carefully investigated structural changes on a $BiFeO_3$ powder sample. In contrast to recent work of Palai *et al.*,[15] we never reached the cubic phase because the decomposition of the sample occurs before. This discrepancy could arise from the presence of some defects probably at the grain boundaries. In agreement with Palai *et al.*, we confirm that the phase above T_c is not cubic. However, our investigation shows that this phase is well refined with a monoclinic with either $P2_1/m$ or $C2/m$ space group rather than an orthorhombic one. This phase is centrosymmetric and characterized by a strong oxygen octahedra tilting along the *b* axis and a metric of the unit cell very close to a tetragonal one. The centrosymmetry imposes the phase to be macroscopically nonferroelectric, even if antiferroelectric displacements of the Fe cations are observed. Our results also evidence a lamellar structure, due to two different BiO_{12} cages, wherein each layer is controlled by the bismuth polyhedron that alternates along the *b* axis, and suggesting a significant electronic rearrangement in terms of chemical bonding, which in turn might condition anisotropic electronic properties. Such lamellar structure provides also an understanding of why BFO decomposes suddenly at high temperature. Moreover, there is no group/subgroup relationship between the $R3c$ and $P2_1/m$ space groups. Such feature explains why the phase transition is not soft-mode driven. Besides, we also demonstrate a first-order-like phase transition. Indeed, the temperature dependence of the lattice parameter displays a strong volume variation at T_c of about 1.4%. Another change is also clearly detected at T_N revealing a spin-lattice coupling related to the appearance of the magnetic structure.

ACKNOWLEDGMENTS

B.D., J.K., and R.H. wish to thank J. Scott for interesting and fruitful discussions. R.H. thanks Celine Byl (LEMHE, ICMMO) for DSC technical assistant. Financial support by the Agence Nationale de la Recherche (PROPER) is gratefully acknowledged. J.K. thanks the European network of excellence FAME and the European STREP MaCoMuFi for financial support. L.B. thanks the NSF under Grants No. DMR-0701558, No. DMR-0080054 (C-SPIN), and No. DMR-0404335, ONR under Grants No. N00014-04-1-0413 and No. N00014-08-1-0915, and DOE under Grant No. DE-FG02-05ER46188 for financial support.

*Present address: Mads Clausen Institute for Product Innovation, University of Southern Denmark, Alsion 2, DK-6400 Sønderborg, Denmark.

[1] G. A. Smolenskii and I. E. Chupis, Sov. Phys. Usp. **25**, 4751 (1982).
[2] H. Schmid, Ferroelectrics **162**, 19 (1994).
[3] J. Wang, J. B. Neaton, H. Zheng, V. Nagarajan, S. B. Ogale, B. Liu, D. Viehland, V. Vaithyanathan, D. G. Schlom, U. V. Waghmare, N. A. Spaldin, K. M. Rabe, M. Wuttig, and R. Ramesh, Science **299**, 1719 (2003).
[4] M. Fiebig, J. Phys. D **38**, R123 (2005).
[5] R. Ramesh and N. Spaldin, Nature Mater. **6**, 21 (2007).
[6] A. M. Kadomtseva, Yu. F. Popov, A. P. Pyatakov, G. P. Vorob'ev, À. Ê. Zvezdin, and D. Viehland, Phase Transitions **79**, 1019 (2006).
[7] P. Fischer, M. Polomka, I. Sosnowska, and M. Szymanski, J. Phys. C **13**, 1931 (1980).
[8] S. V. Kiselev, R. P. Ozerov, and G. S. Zhdanov, Sov. Phys. Dokl. **7**, 742 (1963).
[9] G. A. Smolenskii, V. A. Isupov, N. N. Krainik, and A. I. Agranovskaya, Sov. Phys. Solid State **2**, 2651 (1961).
[10] B. Ruette, S. Zvyagin, A. P. Pyatakov, A. Bush, J. F. Li, V. I. Belotelov, A. K. Zvezdin, and D. Viehland, Phys. Rev. B **69**, 064114 (2004).
[11] G. A. Smolenskii, V. A. Isupov, and N. N. Krainik, Sov. Phys. Solid State **2**, 2651 (1961).
[12] J. R. Teague, R. Gerson, and W. J. James, Solid State Commun. **8**, 1073 (1970).
[13] I. A. Kornev, S. Lisenkov, R. Haumont, B. Dkhil, and L. Bellaiche, Phys. Rev. Lett. **99**, 227602 (2007).
[14] V. V. Shvartsman, W. Kleemann, R. Haumont, and J. Kreisel, Appl. Phys. Lett. **90**, 172115 (2007).
[15] R. Palai, R. S. Katiyar, H. Schmid, P. Tissot, S. J. Clark, J. Robertson, S. A. T. Redfern, G. Catalan, and J. F. Scott, Phys. Rev. B **77**, 014110 (2008).
[16] J. D. Bucci, B. K. Robertson, and W. J. James, J. Appl. Crystallogr. **5**, 187 (1972).
[17] S. A. Fedulov, Sov. Phys. Dokl. **6**, 729 (1962); S. A. Fedulov, N. Yu. Venevtsev, G. S. Zhdanov, E. G. Smazhevskaya, and I. S. Rez, Sov. Phys. Crystallogr. **7**, 62 (1962).
[18] N. N. Kranik, N. P. Khuchua, V. V. Zhdanov, and V. A. Evseev, Sov. Phys. Solid State **8**, 654 (1966).
[19] I. G. Ismailzade, Sov. Phys. Dokl. **11**, 747 (1967).
[20] A. M. Glazer, Acta Crystallogr., Sect. B: Struct. Crystallogr. Cryst. Chem. **28**, 3384 (1972).
[21] H. Béa, M. Bibes, S. Fusil, K. Bouzehouane, E. Jacquet, K. Rode, P. Bencok, and A. Barthélémy, Phys. Rev. B **74**, 020101(R) (2006); H. Béa, M. Bibes, S. Petit, J. Kreisel, and A. Barthélémy, Philos. Mag. Lett. **87**, 165 (2007).
[22] M. K. Singh, H. M. Jang, S. Ryu, and M.-H. Jo, Appl. Phys.

Lett. **88**, 042907 (2006).
[23] M. K. Singh, S. Ryu, and H. M. Jang, Phys. Rev. B **72**, 132101 (2005).
[24] N. N. Kranik, N. P. Khuchua, V. V. Zhdanov, and V. A. Evseev, Sov. Phys. Solid State **8**, 654 (1966); M. M. Kumar, V. R. Palkar, K. Srinivas, and S. V. Suryanarayana, Appl. Phys. Lett. **76**, 2764 (2000); S. T. Zhang, M. H. Lu, D. Wu, Y. F. Chen, and N. B. Ming, *ibid.* **87**, 262907 (2005); G. L. Yuan and S. W. Or, *ibid.* **88**, 062905 (2006); D. H. Wang, L. Yan, C. K. Ong, and Y. W. Du, *ibid.* **89**, 182905 (2006); M. I. Morozov, N. A. Lomanova, and V. V. Gusarov, Russ. J. Gen. Chem. **73**, 1676 (2003).
[25] E. I. Speranskaya, V. M. Skorikov, E. Ya. Rode, and V. A. Terekhova, Izv. Akad. Nauk SSSR [Khim] **5**, 905 (1965) [Bull. Acad. Sci. USSR, Div. Chem. Sci. **14**, 873 (1965)].
[26] J. F. Bérar, IUCr. Satellite Meeting on Powder Diffractometry, Toulouse, France, 1990 (unpublished).
[27] *International Tables for Cyrstallography* (Kluwer, Dordrecht, 1992).
[28] F. Kubel and H. Schmid, Acta Crystallogr., Sect. B: Struct. Sci. **46**, 698 (1990).
[29] H. T. Stokes, E. H. Kishi, D. M. Hatch, and C. J. Howard, Acta Crystallogr., Sect. B: Struct. Sci. **58**, 934 (2002).
[30] R. Haumont, J. Kreisel, and P. Bouvier, Phase Transitions **79**, 1043 (2006); R. Haumont, J. Kreisel, P. Bouvier, and F. Hippert, Phys. Rev. B **73**, 132101 (2006).
[31] S. Kamba, D. Nuzhnyy, M. Savinov, J. Šebek, J. Petzelt, J. Prokleška, R. Haumont, and J. Kreisel, Phys. Rev. B **75**, 024403 (2007).
[32] A. Palewicz, T. Szumiata, R. Przeniosło, I. Sosnowska, and I. Margiolaki, Solid State Commun. **140**, 359 (2006).
[33] A. Palewicz, R. Przenioslo, I. Sosnowska, and A. W. Hewat, Acta Crystallogr., Sect. B: Struct. Sci. **63**, 537 (2007).